

Guaranteed lower eigenvalue bounds for the biharmonic equation

Carsten Carstensen · Dietmar Gallistl

Received: 10 October 2012 / Revised: 26 March 2013 / Published online: 22 May 2013
© Springer-Verlag Berlin Heidelberg 2013

Abstract The computation of lower eigenvalue bounds for the biharmonic operator in the buckling of plates is vital for the safety assessment in structural mechanics and highly on demand for the separation of eigenvalues for the plate's vibrations. This paper shows that the eigenvalue provided by the nonconforming Morley finite element analysis, which is perhaps a lower eigenvalue bound for the biharmonic eigenvalue in the asymptotic sense, is not always a lower bound. A fully-explicit error analysis of the Morley interpolation operator with all the multiplicative constants enables a computable guaranteed lower eigenvalue bound. This paper provides numerical computations of those lower eigenvalue bounds and studies applications for the vibration and the stability of a biharmonic plate with different lower-order terms.

Mathematics Subject Classification (2000) 65N25 · 65N30 · 74K20

Dedicated to Dietrich Braess on the occasion of his 75th birthday.

This work was supported by the DFG Research Center MATHEON.

C. Carstensen (✉) · D. Gallistl
Institut für Mathematik, Humboldt-Universität zu Berlin,
Unter den Linden 6, 10099 Berlin, Germany
e-mail: cc@math.hu-berlin.de

D. Gallistl
e-mail: gallistl@math.hu-berlin.de

C. Carstensen
Department of Computational Science and Engineering, Yonsei University,
120-749 Seoul, Korea

1 Introduction

The Morley nonconforming finite element method provides asymptotic lower eigenvalue bounds for the problem $\Delta^2 u = \lambda u$. It is observed in the numerical examples [8, p.39] that the Morley eigenvalue λ_M is a lower bound of λ . The possible conjecture that this is always the case, however, is false in general. This motivates the task to compute a guaranteed lower eigenvalue bound for all and even the very coarse triangulations based on the Morley finite element discretisation. This paper provides a guaranteed lower bound

$$\lambda_M / (1 + \varepsilon^2 \lambda_M) \leq \lambda \tag{1.1}$$

for a computable value of ε which depends on the maximal mesh-size H and the type of the lower-order term, e.g., $\varepsilon = 0.2574 H^2$ for the eigenvalue problem $\Delta^2 u = \lambda u$.

Let $\Omega \subset \mathbb{R}^2$ be a bounded Lipschitz domain with polygonal boundary $\partial\Omega$ and outer unit normal ν . The boundary is decomposed in clamped (Γ_C), simply supported (Γ_S), and free (Γ_F) parts

$$\partial\Omega = \Gamma_C \cup \Gamma_S \cup \Gamma_F$$

such that Γ_C and $\Gamma_C \cup \Gamma_S$ are closed sets. The vector space of admissible functions reads

$$V := \left\{ v \in H^2(\Omega) \mid v|_{\Gamma_C \cup \Gamma_S} = 0 \text{ and } (\partial\nu/\partial\nu)|_{\Gamma_C} = 0 \right\}.$$

Provided the boundary conditions are imposed in such a way that the only affine function in V is identically zero, $V \cap P_1(\Omega) = \{0\}$, the space V equipped with the scalar product

$$a(v, w) := \int_{\Omega} D^2 v : D^2 w \, dx \quad \text{for all } v, w \in V$$

is a Hilbert space (colon denotes the usual scalar product of 2×2 matrices) with energy norm $\|\cdot\| := a(\cdot, \cdot)^{1/2}$. Given a scalar product b on V with norm $\|\cdot\| := b(\cdot, \cdot)^{1/2}$, the weak form of the biharmonic eigenvalue problem seeks eigenpairs $(\lambda, u) \in \mathbb{R} \times V$ with $\|u\| = 1$ and

$$a(u, v) = \lambda b(u, v) \quad \text{for all } v \in V. \tag{1.2}$$

For a regular triangulation \mathcal{T} of Ω with vertices \mathcal{N} and edges \mathcal{E} suppose that the interior of each boundary edge is contained in one of the parts Γ_C , Γ_S , or Γ_F , and let the piecewise action of the operators ∇ and D^2 be denoted by ∇_{NC} and D^2_{NC} . The space of piecewise polynomials of total (resp. partial) degree k reads $P_k(\mathcal{T})$ (resp. $Q_k(\mathcal{T})$). The Morley finite element space [4] with respect to a regular triangulation \mathcal{T} of Ω equals

$$V_M := \left\{ v_M \in P_2(\mathcal{T}) \mid \begin{array}{l} v_M \text{ is continuous at the interior vertices} \\ \text{and vanishes at the vertices of } \Gamma_C \cup \Gamma_S; \\ \nabla_{NC} v_M \text{ is continuous at the interior edges' midpoints} \\ \text{and vanishes at the midpoints of the edges of } \Gamma_C \end{array} \right\}.$$

The finite element formulation of (1.2) is based on the discrete scalar product

$$a_{NC}(v_M, w_M) := \int_{\Omega} D_{NC}^2 v_M : D_{NC}^2 w_M \, dx \quad \text{for all } v_M, w_M \in V_M$$

and some extension b_{NC} of b to the space $V + V_M$ with norm $\|\cdot\|_{NC} := b_{NC}(\cdot, \cdot)^{1/2}$. It seeks eigenpairs $(\lambda_M, u_M) \in \mathbb{R} \times V_M$ such that $\|u_M\|_{NC} = 1$ and

$$a_{NC}(u_M, v_M) = \lambda_M b_{NC}(u_M, v_M) \quad \text{for all } v_M \in V_M. \tag{1.3}$$

The a priori error analysis can be found in [8]. For conforming finite element discretisations, the Rayleigh-Ritz principle [5], e.g., for the first eigenvalue

$$\lambda = \min_{v \in V \setminus \{0\}} \|v\|^2 / \|v\|_{NC}^2,$$

immediately results in upper bounds for the eigenvalue λ . In many cases it is observed that nonconforming finite element methods provide lower bounds for λ and the paper [10] proves that the eigenvalues of the Morley FEM converge asymptotically from below in the case $b(\cdot, \cdot) = (\cdot, \cdot)_{L^2(\Omega)}$. This paper provides a counterexample to the possible conjecture that λ_M is always a lower bound for λ and provides the guaranteed lower bound (1.1) for a known mesh-size function ε . The main result, Theorem 1, implies (1.1) for any regular triangulation \mathcal{T} with maximal mesh-size H and $\varepsilon = 0.2574 H^2$. Theorem 2 provides lower bounds for higher eigenvalues.

The main tool for the explicit determination of ε is the L^2 error estimate for the Morley interpolation operator from Theorem 3, which also opens the door to guaranteed error control for the Morley finite element discretisation of the biharmonic problem $\Delta^2 u = f$. In comparison with the profound numerical experiments in [8], the theoretical findings of this paper allow guaranteed lower eigenvalue bounds via some immediate postprocessing on coarse meshes with reasonable accuracy even for mediocre refinements.

The remaining parts of the paper are organised as follows. Section 2 discusses the mentioned counterexample and shows that the Morley eigenvalue λ_M may be larger than λ . Section 3 establishes lower bounds for eigenvalues based on abstract assumptions on the Morley interpolation operator I_M . Section 4 provides L^2 error estimates for I_M with explicit constants that enable the results of Sect. 3 for different fourth-order eigenvalue problems. Section 5 presents applications to vibrations and buckling of plates with numerical results for various boundary conditions in the spirit of [8].

Throughout this paper, standard notation on Lebesgue and Sobolev spaces and their norms and the L^2 scalar product $(\cdot, \cdot)_{L^2(\Omega)}$ is employed. The integral mean is denoted by \bar{f} ; the dot (resp. colon) denotes the Euclidean scalar product of vectors (resp. matrices). The measure $|\cdot|$ is context-sensitive and refers to the number of elements of some finite set or the length $|E|$ of an edge E or the area $|T|$ of some domain T and not just the modulus of a real number or the Euclidean length of a vector.

2 Counterexample

The following counterexample shows that the possible conjecture that the Morley FEM always provides lower bounds is wrong. On the coarse triangulation of the square domain $\Omega := (0, 1) \times (0, 1)$ from Fig. 1a, the discrete eigenvalue for clamped boundary conditions $\partial\Omega = \Gamma_C$ computed by the Morley FEM is $\lambda_M = 1.859 \times 10^3$. The discrete eigenvalue computed by conforming FEMs is an upper bound for any lower bound of λ . A computation with the conforming Bogner-Fox-Schmit bicubic finite element method leads to the first eigenvalue $\lambda_{\text{BFS}} = 1.367 \times 10^3$ on the partition from Figure 1b. Hence, λ_M cannot be a lower bound for λ . Table 1 contains the values for finer meshes and shows the convergence behaviour. The results of the subsequent sections lead to the guaranteed lower eigenvalue bounds of Table 1.

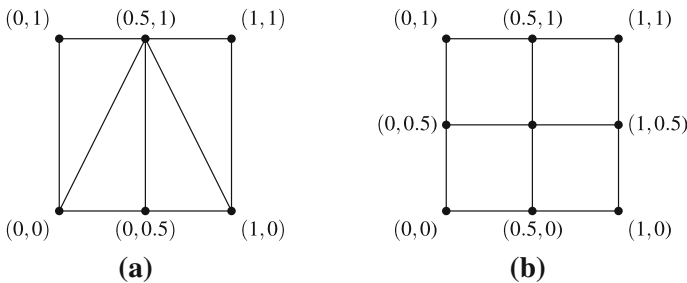


Fig. 1 Meshes for the counterexample for lower bounds. **a** Morley **b** BFS

Table 1 Eigenvalues and number of degrees of freedom for the Morley and Bogner-Fox-Schmit finite element approximations of $\Delta^2 u = \lambda u$

Lower bound	<i>ndof</i> Morley	λ_M	λ_{BFS}	<i>ndof</i> BFS
9.6054	3	1,859.9439	1,367.8580	4
115.2848	21	454.3256	1,300.1260	36
608.8860	105	807.9014	1,295.3400	196
1,079.3590	465	1,109.6437	1,294.9632	900
1,238.6288	1,953	1,241.0582	1,294.9359	3,844
1,280.6944	8,001	1,280.8565	1,294.9341	15,876
1,291.3626	32,385	1,291.3729	1,294.9340	64,516
1,294.0403	130,305	1,294.0410	1,294.9340	260,100

3 Lower eigenvalue bounds

This section establishes lower bounds for eigenvalues. The main tool is the Morley interpolation operator $I_M : V \rightarrow V_M$, which acts on any $v \in V$ by

$$(I_M v)(z) = v(z) \quad \text{for each vertex } z \in \mathcal{N},$$

$$\frac{\partial I_M v}{\partial \nu_E}(\text{mid}(E)) = \int_E \nabla v \cdot \nu_E \, ds \quad \text{for each edge } E \in \mathcal{E},$$

where, for any $E \in \mathcal{E}$, the unit normal vector ν_E has some fixed orientation and the midpoint of E is denoted by $\text{mid}(E)$. For any triangle T and $v \in H^2(T)$, an integration by parts proves the integral mean property for the second derivatives

$$D^2 I_M v = \int_T D^2 v \, dx.$$

With the L^2 projection $\Pi_0 : L^2(\Omega) \rightarrow P_0(\mathcal{T})$, this results in the global identity

$$D_{\text{NC}}^2 I_M = \Pi_0 D^2. \tag{3.1}$$

The main assumption for guaranteed lower eigenvalue bounds is the following approximation assumption for some $\varepsilon > 0$ which depends only on the triangulation and the boundaries $\Gamma_C, \Gamma_S, \Gamma_F$. Suppose

$$\|v - I_M v\|_{\text{NC}} \leq \varepsilon \|v - I_M v\|_{\text{NC}} \quad \text{for all } v \in V. \tag{A}$$

(The proof of (A) follows in Sect. 4 for various boundary conditions.)

Theorem 1 (Guaranteed lower bound for the first eigenvalue) *Under the assumption (A) with parameter $0 < \varepsilon < \infty$, the first eigenpair $(\lambda, u) \in \mathbb{R} \times V$ of the biharmonic operator and its discrete Morley FEM approximation $(\lambda_M, u_M) \in \mathbb{R} \times V_M$ satisfy*

$$\frac{\lambda_M}{1 + \varepsilon^2 \lambda_M} \leq \lambda.$$

Proof The Rayleigh-Ritz principle on the continuous level and the projection property (3.1) for the Morley interpolation operator yield with the Pythagoras theorem

$$\lambda = \|u\|^2 = \|u - I_M u\|_{\text{NC}}^2 + \|I_M u\|_{\text{NC}}^2.$$

The Rayleigh-Ritz principle in the discrete space V_M implies

$$\|u - I_M u\|_{\text{NC}}^2 + \lambda_M \|I_M u\|_{\text{NC}}^2 \leq \lambda. \tag{3.2}$$

The Cauchy inequality plus $\|u\| = 1$ prove

$$b_{\text{NC}}(u - I_M u, u) \leq \|u - I_M u\|_{\text{NC}}.$$

Hence, the binomial formula and the Young inequality reveal for any $0 < \delta \leq 1$

$$\begin{aligned} \|I_M u\|_{NC}^2 &\geq 1 + \|u - I_M u\|_{NC}^2 - 2\|u - I_M u\|_{NC} \\ &\geq 1 - \delta + (1 - \delta^{-1})\|u - I_M u\|_{NC}^2. \end{aligned}$$

Equation (3.2) and (A) lead to

$$\begin{aligned} &\lambda_M \left(1 - \delta + \left(\lambda_M^{-1} + (1 - \delta^{-1})\varepsilon^2 \right) \|u - I_M u\|_{NC}^2 \right) \\ &\leq \|u - I_M u\|_{NC}^2 + \lambda_M (1 - \delta + (1 - \delta^{-1})) \|u - I_M u\|_{L^2(\Omega)}^2 \leq \lambda. \end{aligned}$$

The choice $\delta := \varepsilon^2 \lambda_M / (1 + \varepsilon^2 \lambda_M)$ concludes the proof. □

Theorem 2 (Guaranteed lower bounds for higher eigenvalues) *Under the conditions of Theorem 1 and sufficiently fine mesh-size in the sense that*

$$\varepsilon < \left(\sqrt{1 + J^{-1}} - 1 \right) / \sqrt{\lambda_J}$$

holds for the J -th eigenpair $(\lambda_J, u_J) \in \mathbb{R} \times V$ of the biharmonic operator, the discrete Morley FEM approximation $(\lambda_{M,J}, u_{M,J}) \in \mathbb{R} \times V_M$ satisfies

$$\frac{\lambda_{M,J}}{1 + \varepsilon^2 \lambda_{M,J}} \leq \lambda_J. \tag{3.3}$$

Remark Although the exact eigenvalue λ_J is not known, any upper bound (e.g., by conforming finite element methods) will give a lower bound for the critical mesh-size.

The proof of Theorem 2 employs the following criterion for the linear independence of the Morley interpolants of the first J eigenfunctions.

Lemma 1 *Let $(u_1, \dots, u_J) \in V^J$ be the b -orthonormal system of the first J eigenfunctions and suppose (A) with parameter $\varepsilon < (\sqrt{1 + J^{-1}} - 1) / \sqrt{\lambda_J}$, then the Morley interpolants $I_M u_1, \dots, I_M u_J$ are linearly independent.*

Proof The assumption (A) plus the projection property (3.1) imply for all $j = 1, \dots, J$ that

$$\begin{aligned} \|u_j - I_M u_j\|_{NC} &\leq \varepsilon \|u_j - I_M u_j\|_{NC} \\ &\leq \varepsilon \|u_j\|_{NC} = \varepsilon \sqrt{\lambda_J}. \end{aligned}$$

This and the orthonormality of the eigenfunctions plus the Cauchy inequality show

$$\begin{aligned} &|b_{NC}(I_M u_j, I_M u_k) - b(u_j, u_k)| \\ &= |b_{NC}(u_j - I_M u_j, u_k - I_M u_k) - b_{NC}(u_j - I_M u_j, u_k) - b_{NC}(u_j, u_k - I_M u_k)| \\ &\leq \|u_j - I_M u_j\|_{NC} \|u_k - I_M u_k\|_{NC} + \|u_j - I_M u_j\|_{NC} + \|u_k - I_M u_k\|_{NC} \\ &\leq \varepsilon^2 \lambda_J + 2\varepsilon \sqrt{\lambda_J}. \end{aligned}$$

The condition $\varepsilon < (\sqrt{1 + J^{-1}} - 1)/\sqrt{\lambda_J}$ is equivalent to

$$J(\varepsilon^2 \lambda_J + 2\varepsilon \sqrt{\lambda_J}) < 1.$$

This and the Gershgorin theorem prove that all eigenvalues of the mass matrix

$$\left(b_{\text{NC}}(I_M u_j, I_M u_k) \right)_{j,k=1,\dots,J}$$

are positive. □

Proof of Theorem 2 The Rayleigh-Ritz principle reads

$$\lambda_{M,J} = \min_{\dim V_J=J} \max_{v_M \in V_J \setminus \{0\}} \frac{\|v_M\|_{\text{NC}}^2}{\|v_M\|_{\text{NC}}^2},$$

where the minimum runs over all subspaces $V_J \subset V_M$ with dimension smaller than or equal to J . Lemma 1 guarantees that the vectors $I_M u_1, \dots, I_M u_J$ are linearly independent. Hence, there exist real coefficients ξ_1, \dots, ξ_J with $\sum_{j=1}^J \xi_j^2 = 1$ such that the maximiser of the Rayleigh quotient in $\text{span}\{I_M u_1, \dots, I_M u_J\}$ is equal to $\sum_{j=1}^J \xi_j I_M u_j$. Therefore, $v := \sum_{j=1}^J \xi_j u_j$ satisfies

$$\lambda_{M,J} \leq \frac{\|I_M v\|_{\text{NC}}^2}{\|I_M v\|_{\text{NC}}^2}. \tag{3.4}$$

The projection property (3.1) and the orthogonality of the eigenfunctions prove

$$\|v - I_M v\|_{\text{NC}}^2 + \|I_M v\|_{\text{NC}}^2 = \|v\|^2 = \sum_{j=1}^J \xi_j^2 \lambda_j \leq \lambda_J.$$

This and (3.4) yield

$$\|v - I_M v\|_{\text{NC}}^2 + \lambda_{M,J} \|I_M v\|_{\text{NC}}^2 \leq \lambda_J.$$

This estimate replaces (3.2) in the case of the first eigenvalue. The remaining parts of the proof are identical to the proof of Theorem 1 and, hence, omitted here. □

4 L^2 Error estimate for the Morley interpolation

This section provides error estimates for the Morley interpolation operator with explicit constants to guarantee the approximation assumption (A) of Sect. 3. Let $j_{1,1} = 3.8317059702$ be the first positive root of the Bessel function of the first

kind [6]. The following theorem provides an explicit L^2 interpolation error estimate of the Morley interpolation operator with the constants

$$\begin{aligned}\kappa_{\text{CR}} &:= \sqrt{1/48 + j_{1,1}^{-2}} = 0.298234942888 \quad \text{and} \\ \kappa_{\text{M}} &:= \left(\sqrt{(\kappa_{\text{CR}}^2 + \kappa_{\text{CR}})/12} + \kappa_{\text{CR}}/j_{1,1} \right) = 0.257457844658.\end{aligned}$$

Theorem 3 (Error estimate Morley interpolation) *On any triangle T with diameter $h_T := \text{diam}(T)$, each $v \in H^2(T)$ and its Morley interpolation $I_M v$ satisfy*

$$\begin{aligned}\|v - I_M v\|_{L^2(T)} &\leq \kappa_{\text{M}} h_T^2 \|D^2(v - I_M v)\|_{L^2(T)}, \\ \|\nabla(v - I_M v)\|_{L^2(T)} &\leq \kappa_{\text{CR}} h_T \|D^2(v - I_M v)\|_{L^2(T)}.\end{aligned}$$

The proof of Theorem 3 is based on the following two lemmas.

Lemma 2 (Trace inequality with weights) *Any function $f \in H^1(T)$ on a triangle T with some edge $E \in \mathcal{E}(T)$ satisfies*

$$\begin{aligned}\|f\|_{L^2(E)}^2 &\leq \frac{|E|}{|T|} \|f\|_{L^2(T)}^2 + \frac{h_T |E|}{|T|} \int_T |f| |\nabla f| \, dx \\ &\leq \min_{\alpha > 0} \left(\left(1 + \frac{\alpha}{2}\right) \frac{|E|}{|T|} \|f\|_{L^2(T)}^2 + \frac{h_T^2 |E|}{2\alpha |T|} \|\nabla f\|_{L^2(T)}^2 \right).\end{aligned}$$

Proof Let P denote the vertex opposite to E , such that $T = \text{conv}(E \cup \{P\})$. For any $g \in W^{1,1}(T)$, an integration by parts leads to the trace identity

$$\frac{1}{2} \int_T (\bullet - P) \cdot \nabla g \, dx = \frac{|T|}{|E|} \int_E g \, ds - \int_T g \, dx. \quad (4.1)$$

The estimate $|x - P| \leq h_T$, for $x \in T$, yields for $g = f^2$

$$\|f\|_{L^2(E)}^2 \leq \frac{|E|}{|T|} \|f\|_{L^2(T)}^2 + \frac{h_T |E|}{|T|} \int_T |f| |\nabla f| \, dx.$$

Cauchy and Young inequalities imply, for any $\alpha > 0$, that

$$h_T \int_T |f| |\nabla f| \, dx \leq \frac{h_T^2}{2\alpha} \|\nabla f\|_{L^2(T)}^2 + \frac{\alpha}{2} \|f\|_{L^2(T)}^2.$$

□

Lemma 3 (Friedrichs-type inequality) *On any real bounded interval (a, b) it holds*

$$\max_{f \in H_0^1(a,b)} \frac{\left(\int_a^b f(x) dx\right)^2}{\|f'\|_{L^2(a,b)}^2} = \frac{(b-a)^3}{12}.$$

Proof The bilinear form

$$\langle v, w \rangle := \int_a^b v(x) dx \int_a^b w(x) dx + (b-a)^3 \int_a^b v'(x)w'(x) dx$$

defines a scalar product on $H_0^1(a, b)$ such that $(H_0^1(a, b), \langle \cdot, \cdot \rangle)$ is a Hilbert space. For any $f \in H_0^1(a, b)$ and the quadratic polynomial $p(x) := (x - a)(b - x)$, a straight-forward calculation results in

$$\langle f, p \rangle = \frac{13}{6}(b-a)^3 \int_a^b f(x) dx. \tag{4.2}$$

On the other hand, the Cauchy inequality with respect to the scalar product $\langle \cdot, \cdot \rangle$ reads

$$\begin{aligned} \langle f, p \rangle &\leq \sqrt{\langle f, f \rangle} \sqrt{\langle p, p \rangle} \\ &= \frac{\sqrt{13}}{6}(b-a)^3 \sqrt{\left(\int_a^b f(x) dx\right)^2 + (b-a)^3 \int_a^b f'(x)^2 dx} \end{aligned} \tag{4.3}$$

The combination of (4.2)–(4.3) leads to

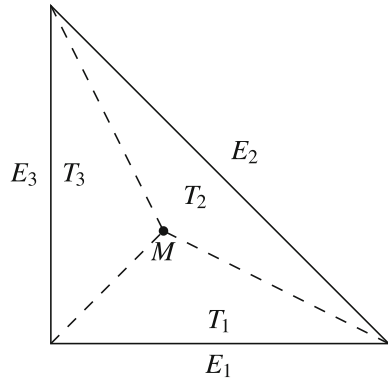
$$12 \left(\int_a^b f(x) dx\right)^2 \leq (b-a)^3 \int_a^b f'(x)^2 dx.$$

The maximum is attained for $f = p$. □

The proof of Theorem 3 makes use of the Crouzeix-Raviart interpolation operator I_{CR} [1, 2]. For a triangle T , the Crouzeix-Raviart interpolation $I_{CR} : H^1(T) \rightarrow P_1(T)$ acts on $v \in H^1(T)$ through

$$I_{CR}v(\text{mid}(E)) = \int_E v ds \quad \text{for all } E \in \mathcal{E}(T)$$

Fig. 2 Subdivision in three subtriangles



and enjoys the integral mean property of the gradient

$$\nabla I_{CR}v = \int_T \nabla v \, dx. \tag{4.4}$$

The following refinement of the results from [3] gives an L^2 error estimate with the explicit constant κ_{CR} from the beginning of this section.

Theorem 4 (L^2 error estimate for Crouzeix-Raviart interpolation) *For any $v \in H^1(T)$ on a triangle T with $h_T := \text{diam}(T)$ the Crouzeix-Raviart interpolation operator satisfies*

$$\|v - I_{CR}v\|_{L^2(T)} \leq \kappa_{CR} h_T \|\nabla(v - I_{CR}v)\|_{L^2(T)}.$$

Proof Let $T = \text{conv}\{P_1, P_2, P_3\}$ with set of edges $\{E_1, E_2, E_3\} = \mathcal{E}(T)$, the barycentre $M := \text{mid}(T)$ and the sub-triangles (see Fig. 2)

$$T_j := \text{conv}\{M, E_j\} \quad \text{for } j = 1, 2, 3.$$

The function $f := v - I_{CR}v$ satisfies, for any edge $E \in \mathcal{E}(T)$,

$$\int_E f \, ds = 0.$$

Let $f_T := \int_T f \, dx$ denote the integral mean on T . The trace identity (4.1) plus the Cauchy inequality reveal for those sub-triangles

$$\begin{aligned} \left| \int_T f \, dx \right| &= \left| \sum_{j=1}^3 \int_{T_j} f \, dx \right| = \left| \frac{1}{2} \sum_{j=1}^3 \int_{T_j} (\bullet - M) \cdot \nabla f \, dx \right| \\ &\leq \frac{1}{2} \|\bullet - M\|_{L^2(T)} \|\nabla f\|_{L^2(T)}. \end{aligned}$$

Let, without loss of generality, $M = 0$ and so $\sum_{j,k=1}^3 P_j \cdot P_k = 0$. An explicit calculation with the local mass matrix $|T|/12(1 + \delta_{jk})_{j,k=1,2,3}$ reveals

$$12|T|^{-1} \|\bullet - M\|_{L^2(T)}^2 = \sum_{j=1}^3 |P_j|^2 = \frac{1}{6} \sum_{j,k=1}^3 |P_j - P_k|^2 \leq h_T^2.$$

Hence,

$$|f_T| \leq \frac{1}{\sqrt{48}|T|^{1/2}} h_T \|\nabla f\|_{L^2(T)} \quad \text{for all } j = 1, 2, 3. \tag{4.5}$$

The Pythagoras theorem yields

$$\|f\|_{L^2(T)}^2 = \|f - f_T\|_{L^2(T)}^2 + |T|f_T^2.$$

The Poincaré inequality with constant $j_{1,1}^{-1}$ from [6] plus (4.5) reveal

$$\|f\|_{L^2(T)}^2 \leq \left(j_{1,1}^{-2} + \frac{1}{48} \right) h_T^2 \|\nabla f\|_{L^2(T_j)}^2.$$

□

Proof of Theorem 3 The triangle inequality reveals for $g := v - I_M v$ that

$$\|g\|_{L^2(T)} \leq \|g - I_{CR}g\|_{L^2(T)} + \|I_{CR}g\|_{L^2(T)}. \tag{4.6}$$

For the first term, Theorem 4 provides the estimate

$$\|g - I_{CR}g\|_{L^2(T)} \leq \kappa_{CR} h_T \|\nabla_{NC}(g - I_{CR}g)\|_{L^2(T)}. \tag{4.7}$$

The integral mean property (4.4) of the gradient allows for a Poincaré inequality

$$\|\nabla_{NC}(g - I_{CR}g)\|_{L^2(T)} \leq h_T/j_{1,1} \|D^2g\|_{L^2(T)}$$

with the first positive root $j_{1,1} = 3.8317059702$ of the Bessel function of the first kind [6]. This controls the first term in (4.6) as

$$\|g - I_{CR}g\|_{L^2(T)} \leq \kappa_{CR} h_T^2/j_{1,1} \|D^2g\|_{L^2(T)}. \tag{4.8}$$

Let $E \in \mathcal{E}(T)$ denote the set of edges of T and let the function $\psi_E \in P_1(T)$ be the Crouzeix-Raviart basis function which satisfies

$$\psi_E(\text{mid } E) = 1 \quad \text{and} \quad \psi_E(\text{mid}(F)) = 0 \quad \text{for } F \in \mathcal{E}(T) \setminus \{E\}.$$

The definition of I_{CR} and the property $\int_T \psi_E \psi_F dx = 0$ for $E \neq F$ prove for the second term in (4.6) that

$$\|I_{CR}g\|_{L^2(T)}^2 = \int_T \sum_{E \in \mathcal{E}(T)} \left(\int_E g ds \right)^2 \psi_E^2 dx = \frac{|T|}{3} \sum_{E \in \mathcal{E}(T)} \left(\int_E g ds \right)^2.$$

Since $g \in H_0^1(E)$ for all $E \in \mathcal{E}(T)$, Lemma 3 implies

$$\left(\int_E g ds \right)^2 \leq \frac{|E|}{12} \|\partial g / \partial s\|_{L^2(E)}^2.$$

By the trace inequality (Lemma 2), this is bounded by

$$\min_{\alpha > 0} \left(\left(1 + \frac{\alpha}{2} \right) \frac{|E|^2}{12|T|} \|\nabla g\|_{L^2(T)}^2 + \frac{h_T^2 |E|^2}{24\alpha |T|} \|D^2 g\|_{L^2(T)}^2 \right).$$

The definition of I_M implies $\nabla I_M v = I_{CR} \nabla v$. Since $\nabla g = \nabla v - I_{CR} \nabla v$, the arguments from (4.7) show

$$\|\nabla g\|_{L^2(T)} \leq \kappa_{CR} h_T \|D^2 g\|_{L^2(T)}.$$

The combination of the preceding four displayed estimates leads to

$$\|I_{CR}g\|_{L^2(T)}^2 \leq \min_{\alpha > 0} \left((1 + \alpha/2) \kappa_{CR}^2 + 1/(2\alpha) \right) \frac{h_T^4}{12} \|D^2 g\|_{L^2(T)}^2. \tag{4.9}$$

The upper bound attains its minimum at $\alpha = 1/\kappa_{CR}$. Altogether, (4.6), (4.8) and (4.9) lead to

$$\|g\|_{L^2(T)} \leq \left(12^{-1/2} \sqrt{\kappa_{CR}^2 + \kappa_{CR}} + \kappa_{CR}/j_{1,1} \right) h_T^2 \|D^2 g\|_{L^2(T)}.$$

□

5 Numerical results

This section provides numerical experiments for the eigenvalue problems

$$\Delta^2 u = \lambda u \quad \text{and} \quad \Delta^2 u = \mu \Delta u \tag{5.1}$$

on convex and nonconvex domains under various boundary conditions.

5.1 Mathematical models

5.1.1 Vibrations of plates

The weak form of the problem $\Delta^2 u = \lambda u$ seeks eigenvalues λ and the deflection $u \in V$ such that

$$a(u, v) = \lambda b(u, v) \quad \text{for all } v \in V$$

for the bilinear form $b(\cdot, \cdot) := (\cdot, \cdot)_{L^2(\Omega)}$. Its Morley finite element discretisation seeks $(\lambda_M, u_M) \in \mathbb{R} \times V_M$ such that

$$a_{NC}(u_M, v_M) = \lambda_M b(u_M, v_M) \quad \text{for all } v_M \in V_M.$$

Theorems 1–3 establish the lower bound J -th eigenvalue

$$\frac{\lambda_{M,J}}{1 + \kappa_M^2 \lambda_{M,J} H^4} \leq \lambda_J$$

for maximal mesh-size $H^2 < (\sqrt{1 + J^{-1}} - 1) / (\kappa_M \sqrt{\lambda_J})$ in case of $J \geq 2$.

5.1.2 Buckling

The weak form of the buckling problem $\Delta^2 u = \mu \Delta u$ seeks a parameter μ and the deflection $u \in V$ such that

$$a(u, v) = \mu b(u, v) \quad \text{for all } v \in V$$

for the bilinear form $b(\cdot, \cdot) := (\nabla \cdot, \nabla \cdot)_{L^2(\Omega)}$. This model describes the critical parameter μ in a stability analysis of a buckling plate loaded with a load in the plate’s mid-surface times μ [9]. Its Morley finite element discretisation seeks $(\mu_M, u_M) \in \mathbb{R} \times V_M$ such that

$$a_{NC}(u_M, v_M) = \mu_M b_{NC}(u_M, v_M) \quad \text{for all } v_M \in V_M$$

with the piecewise version $b_{NC}(\cdot, \cdot) := (\nabla_{NC} \cdot, \nabla_{NC} \cdot)_{L^2(\Omega)}$.

Theorems 1–3 establish the lower bound J -th eigenvalue

$$\frac{\mu_{M,J}}{1 + \kappa_{CR}^2 \mu_{M,J} H^2} \leq \mu_J$$

for maximal mesh-size $H < (\sqrt{1 + J^{-1}} - 1) / (\kappa_{CR} \sqrt{\mu_J})$ in case of $J \geq 2$.

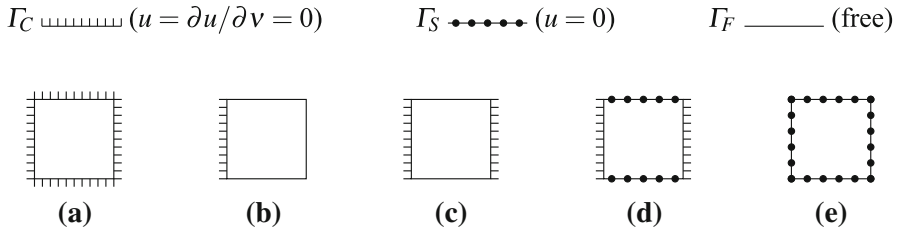
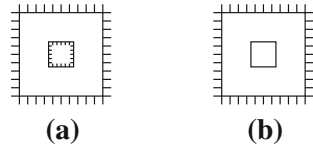


Fig. 3 Boundary conditions for the unit square

Fig. 4 Boundary conditions for the square with hole



5.2 Domains and boundary conditions

The a priori error analysis of the Morley finite element method in [8] has been accompanied by various numerical examples which are easily recast into guaranteed lower bounds via the theoretical findings of this paper. The benchmark examples of this section also consider higher eigenvalues and nonconvex domains.

The domains under consideration are the unit square $\Omega = (0, 1)^2$ and the plate with hole $(0, 1)^2 \setminus ([0.35, 0.65]^2)$. Figure 3 describes the boundary conditions for the unit square, while Fig. 4 shows the boundary conditions for the plate with hole. The different parts of the boundary $\partial\Omega$ are indicated by the following symbols.

5.3 Further remarks on numerical experiments

5.3.1 Numerical realisation

The first eigenvalues of (5.1) are approximated by the Morley FEM (Fig. 5a) on a sequence of successively red-refined triangulations (i.e., each triangle is split into four congruent sub-triangles) based on the initial triangulations of Fig. 6a.

For comparison, the discrete eigenvalues of the conforming Bogner-Fox-Schmit FEM (Fig. 5b) are computed as upper bounds. The conforming finite element space reads $V_{\text{BFS}} := V \cap Q_3(\mathcal{T})$ with the values of the function, its gradient and its mixed second derivative at the free vertices as degrees of freedom as displayed in Fig. 5b. The computations are based on the initial partitions of Fig. 6b.

5.3.2 Higher eigenvalues

To illustrate the result for higher eigenvalues, the tables in 5.4.3 display the approximations for the 20th eigenvalue on the unit square under the boundary conditions 3a and 3e. The required minimal mesh-size for the lower bound according to Theorem 2 leads to $h < 0.016$ (resp. 0.017) for example 3a (resp. 3e), where the upper bounds

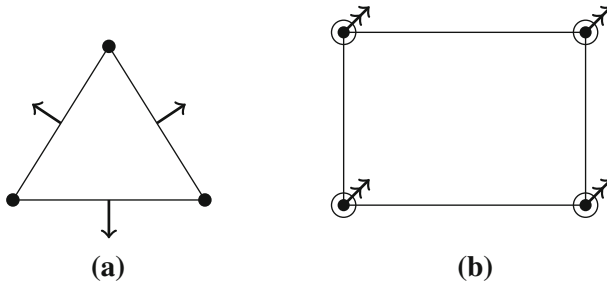


Fig. 5 Morley and Bogner-Fox-Schmit Q_3 finite elements. **a** Morley **b** BFS

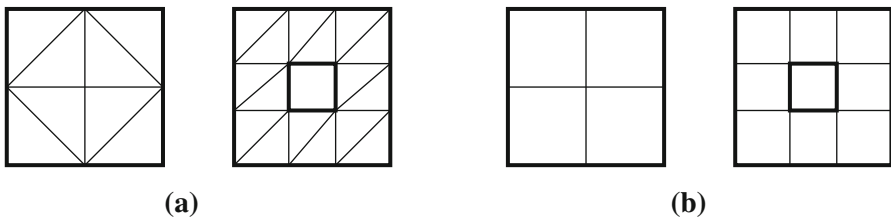


Fig. 6 Initial partitions for the Morley and BFS FEM. **a** Morley **b** BFS

$\lambda_{\text{BFS},20} \geq \lambda$ are used to guarantee a sufficiently fine mesh. This separation condition is satisfied for the last three values of GLB and, therefore, those are valid bounds. (The values in brackets are not necessarily reliable bounds.)

5.3.3 Inexact solve

The estimates from Section 3 are derived under the unrealistic assumption that the discrete algebraic eigenvalue problems are solved exactly. However, since the term $\lambda_M / (1 + \varepsilon^2) \lambda_M$ is monotone in λ_M , any lower bound for the discrete eigenvalue λ_M yields a lower bound for λ . In this sense, this paper reduces the task of guaranteed lower bounds of the eigenvalue problem on the continuous level via the Morley discretisation and sharp interpolation error estimates to the task of guaranteed lower eigenvalue bounds of the algebraic eigenvalue problem in numerical linear algebra. There are many results available for the localisation of eigenvalues in the finite-dimensional algebraic eigenvalue problems in the literature, e.g., in [7]. Throughout this paper and the numerical examples of this section, all numbers provided are computed with the ARPACK and the default parameters.

5.4 Results

The tables display the eigenvalue of the Morley FEM and the guaranteed lower bound (GLB). The eigenvalue of the conforming Bogner-Fox-Schmit FEM is given as an upper bound for comparison. The dash indicates out of memory (8 million degrees of freedom).

5.4.1 First eigenvalue for $\Delta^2 u = \lambda u$ on the unit square

λ_M	GLB	λ_{BFS}
(Boundary condition 3a)		
288.36704	222.04958	1,367.8580
637.14901	611.91175	1,300.1260
1,008.8296	1,004.7288	1,295.3400
1,205.7698	1,205.4022	1,294.9632
1,271.0486	1,271.0230	1,294.9359
1,288.8461	1,288.8444	1,294.9341
1,293.4041	1,293.4039	1,294.9340
1,294.5510	1,294.5509	1,294.9340
1,294.8381	1,294.8380	1,294.9336
(Boundary condition 3b)		
9.4115855	9.3207312	12.480192
11.429097	11.420647	12.374319
12.109523	12.108929	12.363172
12.297560	12.297521	12.362415
12.346044	12.346041	12.362367
12.358275	12.358274	12.362364
12.361341	12.361340	12.362363
12.362103	12.362102	12.362362
12.362252	12.362251	12.362339
(Boundary condition 3c)		
118.46317	105.51708	516.92308
269.41278	264.79492	501.89357
409.86191	409.18341	500.64841
474.00642	473.94961	500.56920
493.62006	493.61620	500.56423
498.80737	498.80712	500.56392
500.12344	500.12342	500.56390
500.45370	500.45369	500.56388
500.53630	500.53629	500.56352
(Boundary condition 3d)		
270.01217	211.00461	870.28523
486.48522	471.63317	840.23446
693.94950	692.00668	838.28577
794.82321	794.66350	838.16022
826.71488	826.70407	838.15227
835.25025	835.24956	838.15177
837.42356	837.42351	838.15174
837.96950	837.96949	838.15171
838.10612	838.10611	838.15136
(Boundary condition 3e)		
239.60730	191.96836	440.00000
323.40541	316.77395	391.31816
368.87652	368.32684	389.74036
384.07793	384.04063	389.64282
388.22057	388.21818	389.63677
389.28068	389.28053	389.63639
389.54733	389.54732	389.63637
389.61409	389.61408	389.63636
389.63075	389.63074	389.63634

5.4.2 First eigenvalue for $\Delta^2 u = \lambda u$ on the square with hole

λ_M	GLB	λ_{BFS}
(Boundary condition 4a)		
6,605.7795	242.12417	31,270.769
7,555.1473	2,624.4604	28,314.668
15,294.185	12,356.931	27,458.216
21,971.980	21,512.833	27,138.816
25,144.874	25,106.547	27,005.952
26,279.553	26,276.932	26,947.608
26,665.404	26,665.235	26,921.219
26,803.927	26,803.916	26,909.085
26,857.825	26,857.824	–
(Boundary condition 4b)		
741.11343	187.68590	1,862.4481
1,246.1046	951.31959	1,855.3809
1,626.2648	1,586.1738	1,851.9814
1,784.0893	1,781.0028	1,850.9178
1,832.2899	1,832.0860	1,850.6129
1,845.5824	1,845.5694	1,850.5473
1,849.1916	1,849.1907	1,850.5479
1,850.1867	1,850.1866	1,850.5609
1,850.4690	1,850.4689	1,850.5712

5.4.3 Higher eigenvalues for $\Delta^2 u = \lambda u$ on the square domain

(Boundary condition 3a)			$H \times 10^{-1}$	(Boundary condition 3e)		
$\lambda_{M,20}$	GLB	$\lambda_{BFS,20}$		$\lambda_{M,20}$	GLB	$\lambda_{BFS,20}$
33,194.719	(938.24364)	180,927.73	35.35	16,884.905	(913.30834)	112,640.00
56,445.852	(12,128.990)	139,642.27	17.67	53,924.215	(12,008.327)	100,177.45
102,198.50	(72,303.616)	138,018.79	8.838	83,810.508	(62,588.541)	99,773.533
125,411.88	(121,557.17)	137,905.04	4.419	94,755.581	(92,538.410)	99,748.561
134,423.04	(134,138.08)	137,897.32	2.209	98,415.381	(98,262.552)	99,747.012
137,002.79	136,984.25	137,896.82	1.104	99,408.352	99,398.592	99,746.916
137,671.63	137,670.45	137,896.79	0.552	99,661.908	99,661.294	99,746.910
137,840.39	137,840.31	137,896.79	0.276	99,725.636	99,725.597	99,746.909

5.4.4 First eigenvalue for $\Delta^2 u = \mu \Delta u$ on the unit square

μ_M	GLB	λ_{BFS}
(Boundary condition 3a)		
30.430781	22.737880	52.923077
46.100761	40.864499	52.576696
50.603228	48.884311	52.362578
51.874002	51.410714	52.345894

μ_M	GLB	λ_{BFS}
52.223278	52.105101	52.344768
52.314035	52.284337	52.344696
52.337005	52.329570	52.344691
52.342768	52.340908	52.344690
52.344208	52.343743	52.344676
(Boundary condition 3b)		
2.4064529	2.3437460	2.4859617
2.4518157	2.4352200	2.4686648
2.4634618	2.4592520	2.4674819
2.4664122	2.4653558	2.4674062
2.4671535	2.4668891	2.4674014
2.4673392	2.4672731	2.4674011
2.4673857	2.4673691	2.4674011
2.4673963	2.4673921	2.4674008
2.4673914	2.4673903	2.4673965
(Boundary condition 3c)		
13.403557	11.665198	33.066754
22.926106	21.552699	32.417350
29.338870	28.752692	32.293439
31.461504	31.290487	32.275273
32.056325	32.011758	32.272463
32.215866	32.204601	32.272026
32.257575	32.254750	32.271958
32.268298	32.267591	32.271947
32.271024	32.270847	32.271931
(Boundary condition 3d)		
24.000000	18.944891	38.176592
32.093424	29.465032	37.880015
36.168341	35.281625	37.805108
37.377276	37.136145	37.799957
37.692922	37.631319	37.799628
37.772852	37.757367	37.799607
37.792911	37.789034	37.799606
37.797931	37.796961	37.799604
37.799185	37.798942	37.799589
(Boundary condition 3e)		
18.334369	15.229883	22.000000
19.443160	18.446280	19.817243
19.667256	19.402101	19.744335
19.721247	19.653913	19.739533
19.734714	19.717814	19.739229
19.738084	19.733854	19.739210
19.738928	19.737870	19.739209
19.739138	19.738873	19.739209
19.739189	19.739122	19.739208

5.4.5 First eigenvalue of $\Delta^2 u = \mu \Delta u$ on the square with hole

μ_M	GLB	μ_{BFS}
(Boundary condition 4a)		
65.836950	27.041396	277.04748
140.00805	79.426405	265.59236
210.08856	163.34921	260.75573
239.26986	221.24527	258.83912
250.18631	244.96933	257.99165
254.32732	252.95825	257.60556
255.99152	255.64335	257.42742
256.69732	256.60970	257.34466
257.00896	256.98699	–
(Boundary condition 4b)		
31.637668	18.726875	43.732101
38.366123	31.733452	42.623655
40.936657	38.774808	42.387116
41.849116	41.261178	42.326353
42.155629	42.004899	42.311264
42.257614	42.219647	42.308505
42.292109	42.282595	42.308707
42.304027	42.301646	42.309345
42.308224	42.307628	42.309833

References

1. Brenner, S.C., Scott, L.R.: The mathematical theory of finite element methods, texts in applied mathematics, vol. 15, 3rd edn. Springer, New York (2008)
2. Carstensen, C., Gedicke, J.: Guaranteed lower bounds for eigenvalues. *Math. Comp.* Accepted for publication (2013)
3. Carstensen, C., Gedicke, J., Rim, D.: Explicit error estimates for Courant, Crouzeix-Raviart and Raviart-Thomas finite element methods. *J. Comput. Math.* **30**(4), 337–353 (2012)
4. Ciarlet, P.G.: The finite element method for elliptic problems. *Studies in Mathematics and its Applications*, vol. 4. North-Holland Publishing Co., Amsterdam (1978)
5. Evans, L.C.: Partial differential equations, Graduate Studies in Mathematics, vol. 19, 2nd edn. American Mathematical Society, Providence (2010)
6. Laugesen, R.S., Siudeja, B.A.: Minimizing Neumann fundamental tones of triangles: an optimal Poincaré inequality. *J. Diff. Equ.* **249**(1), 118–135 (2010)
7. Parlett, B.N.: The symmetric eigenvalue problem, *Classics in Applied Mathematics*, vol. 20. Society for Industrial and Applied Mathematics (SIAM), Philadelphia, PA (1998). Corrected reprint of the 1980 original
8. Rannacher, R.: Nonconforming finite element methods for eigenvalue problems in linear plate theory. *Numer. Math.* **33**(1), 23–42 (1979)
9. Timoshenko, S., Gere, J.: Theory of elastic stability. *Engineering Societies Monographs*. MacGraw-Hill International, New York (1985)
10. Yang, Y., Lin, Q., Bi, H., Li, Q.: Eigenvalue approximations from below using Morley elements. *Adv. Comput. Math.* **36**, 443–450 (2011)